Triplet Excited States of Free-Base Porphin and Its β-Octahalogenated Derivatives†

Kiet A. Nguyen,* Paul N. Day, and Ruth Pachter*

Air Force Research Laboratory, Materials and Manufacturing Directorate, AFRL/MLPJ, Wright-Patterson Air Force Base, Ohio 45433-7702

Received: October 27, 1999; In Final Form: February 7, 2000

Density functional theory (DFT) electronic structure calculations were carried out to predict the structures, energetics, and triplet−triplet (T−T) spectra for the low-lying triplet states of free-base porphin (PH_2) and its β-octahalogenated derivatives (β-PH_2X_8; X = F, Cl, Br). The lowest triplet excited state of PH_2 and β-PH_2X_8 was found to retain D_{2h} symmetry with stretched $C_\beta-C_\beta$ and $C_\beta-C_m$ bond distances. For free-base porphin, the singlet−triplet (S_0-T_1) gap obtained with the B3LYP functional was in excellent agreement with the experimental phosphorescence value. Excitation energies computed by time-dependent DFT also provided a fine account of the observed T−T spectrum. β-Halogenation had little effect on the singlet−triplet gaps of porphin. The S_0-T_1 and S_0-T_2 splittings for β-PH_2X_8 were within 0.1 eV of the corresponding splittings in the unsubstituted porphin. All bands in the T−T spectra of β-PH_2X_8 were predicted to be significantly (up to 0.65 eV) red-shifted in comparison to corresponding bands of the unsubstituted porphin.

I. Introduction

Porphyrins are found in a wide variety of applications that exploit their ground- and excited-state properties. In the triplet excited states, they participate in photoinduced energy- and electron-transfer reactions that are important in photodynamic therapy.[1] Their strong triplet excited-state absorption has also generated considerable interest in the use of porphyrin and its derivatives for nonlinear absorption (NLA)[2−5] and optical storage[6] applications. Since a high transmission under regular laser conditions and a low transmission under high-intensity laser sources is desirable, one of the basic requirements for an NLA chromophore is an excited-state absorption cross section much stronger than that of its ground-state counterpart over a wide spectral range. In porphyrins and related compounds, the mechanisms of NLA have been shown to involve primarily the ground-state singlet−singlet and triplet−triplet (T−T) absorptions, and efficient singlet−triplet intersystem crossing in order to maintain a sufficient triplet population.[2,4] Thus, the prediction of photophysical properties of the triplet excited state are important in the understanding and design of porphyrin-based NLA dyes. However, the electronic structure and T−T spectrum even of the parent free-base porphin (PH_2) are not well understood (Figure 1). There have been numerous experimental[7−11] and theoretical[9,12−14] studies aimed at unraveling the electronic structure and electronic spectrum for the triplet excited states of porphyrins. Previous theoretical studies of the triplet excited states of free-base porphin ($^3PH_2$) have been limited to simple molecular orbital (MO) levels using the ground-state geometry. In these studies, the computed energy separations between the four low-lying triplet states, obtained from the excitation between Gouterman's four orbitals (the two highest occupied MOs and the two lowest occupied virtuals), are very small and their relative ordering is dependent on the choice of parameters. Although it has been recognized that the prediction of the electronic structure of $^3PH_2$ cannot be made on the basis of these semiempirical calculations, an assignment of $^3B_{2u}$ symmetry for the lowest triplet state (T_1) has been made on the basis of such calculations and electron paramagnetic resonance (EPR) spectra.[9] However, a more recent electron−nuclear double resonance (ENDOR) study of $^3PH_2$ has concluded that the EPR interpretation and assignment are erroneous.[15] The ENDOR data pointed to C_{2h} instead of D_{2h} symmetry for T_1 of PH_2.

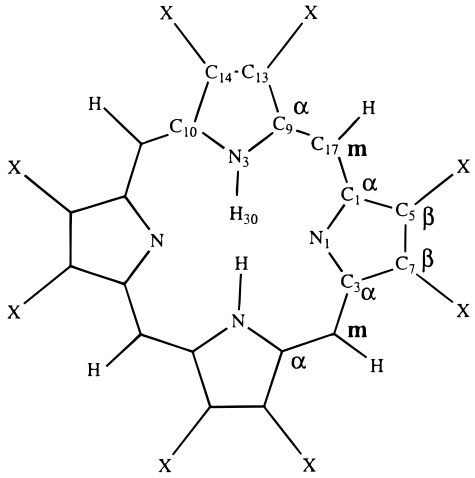

Figure 1. Labeling scheme for free-base porphin.

Early theoretical work on the T−T absorption spectrum of tetraphenylporphyrin predicted a large number of allowed bands. Although quantitative agreement with experiment was not obtained, these Pariser−Parr−Pople (PPP) calculations by Weiss et al.[12] revealed the complex nature of the observed T−T spectrum. These researchers concluded that the four-orbital model proposed by Gouterman[16] is not valid for interpreting the T−T spectra of porphyrins. Recently, semiempirical T−T spectral calculations for porphin have been carried out using the ground-state geometry.[17] Configuration interaction (CI) singles based on the intermediate neglect of differential overlap/spectroscopic (INDO/S) approximations grossly underestimated the T−T excitation energies of porphin. However, the corre-

† Part of the special issue "Electronic and Nonlinear Optical Materials: Theory and Modeling".

10.1021/jp993807q CCC: $19.00
Published on Web 05/03/2000

sponding MRCISDT-CI excitation energies are in reasonable agreement with experimental data.[17] More recently, the versatile Kohn−Sham density functional theory (DFT) and the time-dependent DFT (TDDFT) in particular, have been quite successful in predicting the ground-state (S_0) electronic structures and spectra of porphin[18−24] and the larger tetraphenylporphyrin and its β-octahalogenated derivatives.[25] DFT also provides energetics of excited-state open-shell radical cations[26,27] and triplets of porphyrins[21,25] that are in quantitative agreement with experimental data.

In the present study we describe the results of DFT and TDDFT electronic structure calculations for $^3PH_2$. These calculations were carried out to determine the structures, energetics, and spectra of low-lying triplet states for PH_2. The computed results shed light on the outstanding electronic and structural issues for $^3PH_2$ and its observed spectral data. Good agreement is found between the computed and observed T−T spectra for free-base porphin. In addition, the computed structures, energetics, and T−T spectra for the corresponding β-octahalogenated derivatives (β-PH_2X_8; X = F, Cl, Br) which have not yet been synthesized are presented. These halogenated porphyrins have much larger ionization potentials that can result in greater stability toward direct photodegradations and other photoinduced reactions.[21,26] Furthermore, the triplet population can be effectively modulated by halogenation as reported by Bonnet et al. for a series of free-base octaalkylporphyrins.[28] The T−T spectra of these and other halogenated porphyrins, therefore, are of interest in the design of nonlinear absorption dyes.

II. Computational Methods

The structures have been predicted using Kohn−Sham (KS)[29] density functional theory with the 6-31G(d)[30,31] basis set (for carbon, hydrogen, and fluorine). The effective core potentials and basis sets of Stevens et al.[32,33] were used for heavier elements. DFT calculations were carried out using Becke's three-parameter (B3LYP) hybrid functional.[34−36] Open-shell DFT calculations for the triplets were carried out using the unrestricted self-consistent field (SCF)[37] formalism, while the restricted version[38] was used for the closed-shell species. As typically observed in open-shell DFT calculations, spin contamination of the triplet states is low.[39] The $<S^2>$ values for all triplets are below 2.07. The structures were verified to be either minima or transition states by evaluating the appropriate matrix of energy second derivatives (Hessian). The excitation energy and oscillator strength calculations were carried out using time-dependent density functional theory (TDDFT)[22−24] as implemented in the Gaussian 98[40] program. These TDDFT calculations, carried out at the B3LYP structures, were done with the same basis set used in the DFT structural calculations. For porphin, the more economical local[41] (LSDA) and nonhybrid functionals (BP86[35,42] and PW91[35,43]) have also been used to assess their applicability. In addition, calculations with the larger 6-311+G(2d,p)[44,45] basis set were carried out to gauge the effect of basis set on the energetics.

III. Results and Discussion

A. Structures and Energetics. *1. $^3PH_2$.* The search for metastable triplet states of PH_2 included four electronic states obtained by exciting between Gouterman's four orbitals (the two highest occupied MOs and the two lowest virtuals). These excitations give rise to $^3B_{2u}$ and $^3B_{1u}$ electronic states. The geometrical parameters and relative energies of these four states are listed in Tables 1 and 2. The S_0 structural parameters, computed previously,[21] are also included for comparison. The lowest triplet excited-state structure was found to retain D_{2h} ($^3B_{2u}$) symmetry with a positive definite Hessian. Among the noticeable structural changes upon going from S_0 to T_1 are the stretching (by 0.03 Å) of one of the $C_\beta-C_\beta$ ($C_{14}-C_{13}$) or $C_\alpha-C_m$ (C_9-C_{17}) bonds and the shortening of one of the $C_\alpha-C_\beta$ (C_9-C_{13}) bonds by about the same amount (see Table 1 and Figure 1). Other bond changes involve a slight (0.01 Å) increase and decrease in the N_1-C_3 and C_1-C_{17} distances, respectively. All S_0-T_1 shifts in bond angles are no larger than 1°. Energetically, T_1 lies 1.53 eV (Table 2) above S_0 on the classical potential energy surface (PES). The S_0-T_1 splitting is reduced to 1.42 eV, after zero point energy corrections are included. This value, computed at the B3LYP/6-31G(d) level, compares well with the experimental phosphorescence value of 1.58 eV reported by Gouterman and Khalil.[8] The B3LYP/6-31G(d) results appear to be converged because the S_0-T_1 splitting is improved by only 0.03 eV at the B3LYP/6-311+G(2d,p) level. Basis set corrections, therefore, were not carried out for other systems.

The excitation from HOMO − 1 to LUMO + 1 gives the second $^3B_{2u}(a_u \otimes b_{2g})$ state which has the opposite geometric distortions when compared to T_1. The $C_\beta-C_\beta$ ($C_{14}-C_{13}$) bond decreases by 0.02 Å while the $C_\alpha-C_\beta$ (C_9-C_{13}) bond increases by 0.03 Å in comparison to the corresponding bond distances in S_0 (see Table 1). In addition, there is a slight increase (0.02 Å) in the C_1-C_{17} bond distance. Energetically, the 2^3B_{2u} state is only about 0.4 eV above T_1. However, the 2^3B_{2u} structure is

TABLE 1: Geometry Parameters (in Angstroms and Degrees) for the Ground and Triplet Excited States of Free-Base Porphin

	^1A_g	1^3B_{2u} ($b_{3u} \otimes b_{1g}$)	2^3B_{2u} ($a_u \otimes b_{2g}$)	1^3B_{1u} ($b_{3u} \otimes b_{2g}$)	2^3B_{1u} ($a_u \otimes b_{1g}$)
$H_{30}-N_3$	1.015	1.015	1.014	1.015	1.017
N_3-C_9	1.372	1.372	1.381	1.376	1.374
N_1-C_3	1.364	1.372	1.364	1.370	1.371
C_9-C_{13}	1.435	1.408	1.461	1.438	1.432
C_5-C_1	1.460	1.463	1.455	1.435	1.481
$C_{14}-C_{13}$	1.372	1.401	1.354	1.370	1.380
C_5-C_7	1.356	1.353	1.363	1.376	1.344
C_9-C_{17}	1.394	1.428	1.372	1.391	1.410
C_1-C_{17}	1.400	1.389	1.420	1.420	1.391
$C_{13}-H$	1.082	1.082	1.082	1.082	1.082
C_5-H	1.083	1.083	1.083	1.083	1.083
$C_{17}-H$	1.086	1.087	1.086	1.087	1.085
$\alpha(H_{30}-N_3-C_9)$	124.6	124.9	124.4	124.6	124.6
$\alpha(C_9-N_3-C_{10})$	110.9	110.3	111.1	110.7	110.7
$\alpha(C_1-N_1-C_3)$	105.4	105.4	105.3	105.0	105.5
$\alpha(N_3-C_9-C_{13})$	106.5	107.3	106.0	106.5	106.7
$\alpha(N_1-C_1-C_5)$	111.1	110.8	111.3	111.4	110.9
$\alpha(C_9-C_{13}-C_{14})$	108.0	107.6	108.4	108.1	107.9
$\alpha(C_1-C_5-C_7)$	106.2	106.5	106.1	106.1	106.3
$\alpha(N_3-C_9-C_{17})$	125.5	124.6	126.8	125.8	125.1
$\alpha(N_1-C_1-C_{17})$	125.5	125.1	124.8	123.7	126.7
$\alpha(C_9-C_{17}-C_1)$	127.1	128.1	126.6	128.4	126.3
$\alpha(C_9-C_{13}-H)$	124.3	124.9	123.7	124.2	124.3
$\alpha(C_1-C_5-H)$	125.4	125.2	125.5	125.8	124.9
$\alpha(C_9-C_{17}-H)$	115.9	115.0	116.5	115.3	116.1

TABLE 2: B3LYP/6-31G(d) Adiabatic ($S_0 \rightarrow T_1$) Excitation Energies (in eV) for Free-Base Porphin

electronic states	ΔE	ΔH_0
$1^3B_{2u}(b_{3u} \otimes b_{1g})$	1.53	1.42[a]
$2^3B_{2u}(a_u \otimes b_{2g})$	1.88	1.70[b]
$1^3B_{1u}(b_{3u} \otimes b_{2g})$	1.78	1.78
$2^3B_{1u}(a_u \otimes b_{1g})$	2.03	1.94[c]

[a] Experimental phosphorescence value of 1.58 eV.[8] [b] Excluding one imaginary frequency of 4199i cm^{-1}. [c] Excluding one imaginary frequency of 323i cm^{-1}.

TABLE 3: Geometry Parameters (in Angstroms and Degrees) for the Ground and Excited Triplet States of Free-Base β-Halogenated Porphyrins

	PH_2F_8			PH_2Cl_8			PH_2Br_8		
	^1A_g	$^3B_{2u}$	$^3B_{1u}$	^1A_g	$^3B_{2u}$	$^3B_{1u}$	^1A_g	$^3B_{2u}$	$^3B_{1u}$
$H_{30}-N_3$	1.015	1.014	1.014	1.015	1.015	1.015	1.016	1.015	1.015
N_3-C_9	1.374	1.374	1.377	1.372	1.372	1.375	1.372	1.372	1.375
N_1-C_3	1.365	1.374	1.371	1.362	1.371	1.369	1.363	1.372	1.369
C_9-C_{13}	1.433	1.405	1.436	1.439	1.410	1.442	1.440	1.411	1.443
C_5-C_1	1.454	1.458	1.429	1.463	1.466	1.435	1.464	1.467	1.436
$C_{14}-C_{13}$	1.369	1.397	1.367	1.375	1.404	1.373	1.374	1.404	1.373
C_5-C_7	1.353	1.350	1.370	1.358	1.356	1.377	1.359	1.356	1.377
C_9-C_{17}	1.390	1.424	1.386	1.390	1.424	1.387	1.390	1.424	1.387
C_1-C_{17}	1.396	1.384	1.417	1.397	1.385	1.417	1.397	1.386	1.417
C_{13}-X	1.331	1.335	1.331	1.724	1.727	1.723	1.878	1.880	1.876
C_5-X	1.336	1.335	1.341	1.729	1.727	1.733	1.882	1.881	1.886
$C_{17}-H$	1.085	1.086	1.086	1.084	1.085	1.085	1.084	1.085	1.085
$\alpha(H_{30}-N_3-C_9)$	124.3	124.5	124.3	124.2	124.4	124.2	124.2	124.4	124.3
$\alpha(C_9-N_3-C_{10})$	111.5	111.1	111.3	111.7	111.2	111.5	111.6	111.1	111.5
$\alpha(C_1-N_1-C_3)$	106.0	105.9	105.8	106.4	106.3	106.0	106.5	106.4	106.1
$\alpha(N_3-C_9-C_{13})$	105.9	106.5	105.9	106.0	106.7	106.1	106.1	106.7	106.1
$\alpha(N_1-C_1-C_5)$	110.5	110.2	110.5	110.4	110.2	110.6	110.4	110.2	110.6
$\alpha(C_9-C_{13}-C_{14})$	108.3	108.0	108.4	108.1	107.7	108.2	108.1	107.7	108.2
$\alpha(C_1-C_5-C_7)$	106.5	106.8	106.6	106.4	106.7	106.4	106.4	106.7	106.4
$\alpha(N_3-C_9-C_{17})$	126.5	125.8	126.8	126.3	125.5	126.4	126.2	125.3	126.3
$\alpha(N_1-C_1-C_{17})$	126.4	126.0	124.8	126.2	125.8	124.6	126.0	125.7	124.5
$\alpha(C_9-C_{17}-C_1)$	125.8	126.6	126.9	126.6	127.5	127.7	126.9	127.8	128.0
$\alpha(C_9-C_{13}$-X)	123.8	124.9	123.6	124.8	125.7	124.7	124.7	125.6	124.6
$\alpha(C_1-C_5$-X)	124.4	124.0	124.9	126.0	125.6	126.2	126.1	125.7	126.2
$\alpha(C_9-C_{17}-H)$	116.7	115.9	116.2	116.2	115.3	115.8	116.0	115.2	115.6

not a minimum, but a saddle point on the PES with an imaginary frequency of 4199i cm^{-1} whose normal mode leads to a C_{2h} structure with inequivalent C−N distances.

The second triplet excited state (T_2) of porphin, $1^3B_{1u}(b_{3u} \otimes b_{2g})$, is obtained from the HOMO to LUMO + 1 excitation. This is a true metastable state with a positive definite Hessian. T_2 is predicted to lie 1.78 eV above the ground state resulting in a T_1-T_2 splitting of only 0.25 eV (Table 2). Structurally, going from T_1 to T_2 involves shortening of one $C_\alpha-C_\beta$ (0.03 Å, C_1-C_5) and lengthening (0.03−0.04 Å) of the other $C_\alpha-C_\beta$ (C_9-C_{13}) and the $C_\alpha-C_m$ (C_1-C_{17} and C_9-C_{17}) bonds. The stretched $C_\beta-C_\beta$ ($C_{14}-C_{13}$) in $1^3B_{1u}(b_{3u} \otimes b_{2g})$ is shortened while the other $C_\beta-C_\beta$ (C_5-C_7) is lengthened (see Table 1 and Figure 1). The second $^3B_{1u}(a_u \otimes b_{1g})$ state is obtained from the HOMO - 1 to LUMO + 1 excitation. This structure, lying 2.03 eV above S_0 with an imaginary frequency of 323i cm^{-1}, is not a minimum on the PES. The imaginary frequency of $2^3B_{1u}(a_u \otimes b_{1g})$ also has a normal mode leading to a structure with C_{2h} symmetry. Following the imaginary normal modes, the macrocyclic ring was allowed to distort to C_{2h} symmetry. The lowest energy state (^3B_u) converged to the T_1 (D_{2h}, 1^3B_{2u}) structure after geometry optimization. Other electronic states (^3A_u, ^3A_g, and ^3B_g) lie significantly higher in energy. Frequency calculations, therefore, were not carried out for these high-energy C_{2h} structures. Optimizing the triplet under C_{2v} also leads to a D_{2h} structure (T_1) found earlier.

2. $^3\beta$-PH_2X_8. The geometrical parameters and relative energies of $^3\beta$-PH_2X_8 for the 1^3B_{2u} and 1^3B_{1u} states are listed in Tables 3 and 4. The ground-state geometries[21] are also included for comparison. Other higher electronic states that were unstable in $^3PH_2$ were not considered for $^3\beta$-PH_2X_8. These β-halogenated porphyrins apparently undergo excited-state distortion in a fashion similar to the parent porphin system. All β-PH_2X_8 are predicted to have stable D_{2h} structures for both the 1^3B_{2u} and 1^3B_{1u} states. Similar to $^3PH_2$, the lowest triplet excited states for all $^3\beta$-PH_2X_8 are of $^3B_{2u}$ symmetry. The structural changes in the porphyrin skeleton going from S_0 to T_1 for β-PH_2X_8, not surprisingly, are almost identical to those found in PH_2. The porphyrin skeletons of the triplet states of β-PH_2X_8, therefore, are essentially unaffected by β-halogenation. Energetically, β-halogenation has little effect on the T_1 and T_2 energy levels. The S_0-T_1 and S_0-T_2 splittings for β-PH_2X_8 are within 0.1 eV of the corresponding splittings in the unsubstituted PH_2.

TABLE 4: B3LYP/6-31G(d) Adiabatic ($S_0 \rightarrow T_1$) Excitation Energies (in eV) for Free-Base Porphyrins

	$^3B_{2u}$		$^3B_{1u}$	
system	ΔE	ΔH_0	ΔE	ΔH_0
PH_2	1.53	1.42	1.78	1.78
β-PH_2F_8	1.62	1.41	1.86	1.88
β-PH_2Cl_8	1.52	1.50	1.74	1.78
β-PH_2Br_8	1.50	1.39	1.72	1.77

B. Triplet−Triplet Spectra. *1. $^3PH_2$.* In the previous section, the 1^3B_{2u} state was established as the lowest triplet excited state. We now turn our attention to its T−T absorption spectrum. While a number of ground-state spectral studies are reported for PH_2, studies of its experimental T−T spectrum are limited to those reported by Sapunov et al.[11] and Radziszewski et al.[10] The T−T spectrum of $^3PH_2$ in dimethylphthalate has five bands as shown in Figure 2.[11,46] The low-energy region is broad and low in intensity. Two bands with maxima at 1.56 eV (band I) and 1.65 eV (band II) can be identified in this region. The higher-energy region with a maximum at 2.96 eV (band III) and a shoulder at 2.82 eV (band IV) extends from about 2.5 to 3.1 eV. The fifth band has a maximum at 3.23 eV (band V). In addition to bands reported by Sapunov et al., Radziszewski et al.[10] recorded another transition with a maximum at 4.00 eV (not shown in Figure 2) for $^3PH_2$ in an Ar matrix at 10 K.

Our TDDFT results for the lowest 40 roots reveal 18 allowed transitions (Table 5). It appears that the two experimental low-energy bands at 1.65 and 1.56 eV (a shoulder) are related to the first $^3B_{3g}$ and ^3A_g states, respectively. The 1^3B_{2u} band of 1.56 eV with an oscillator strength of 0.012 is within 0.1 eV of experiment. The 1^3B_{3g} band, predicted to appear at 1.81 eV with a larger oscillator strength (0.034), is overestimated by 0.16 eV.

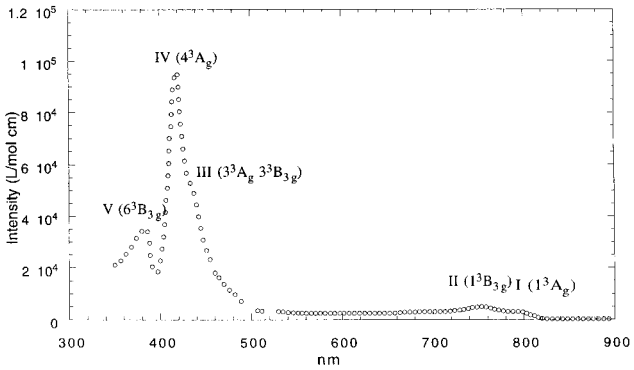

Figure 2. Experimental triplet−triplet (ref 11) absorption spectrum of PH_2.

TABLE 5: T−T Excitation Energies (in eV) and Oscillator Strengths for Free-Base ($^3B_{2u}$) Porphin

transition	excitation energies	oscillator strength	exp
1^3A_g ($\pi \rightarrow \pi^*$)	1.65	0.0120	1.59[a]
1^3B_{3g} ($\pi \rightarrow \pi^*$)	1.81	0.0340	1.65[a]
2^3B_{3g} ($\pi \rightarrow \pi^*$)	2.13	0.0069	
2^3A_g ($\pi \rightarrow \pi^*$)	2.29	0.0029	
1^3B_{1g} ($\pi \rightarrow \pi^*$)	2.43	0.0006	
3^3B_{3g} ($\pi \rightarrow \pi^*$)	2.62	0.0178	
3^3A_g ($\pi \rightarrow \pi^*$)	2.82	0.0145	
4^3B_{3g} ($\pi \rightarrow \pi^*$)	2.87	0.0306	2.82[a]
5^3B_{3g} ($\pi \rightarrow \pi^*$)	3.15	0.0023	
4^3A_g ($\pi \rightarrow \pi^*$)	3.24	0.3253	2.96[a]
6^3B_{3g} ($\pi \rightarrow \pi^*$)	3.54	0.5473	3.23[a]
5^3A_g ($\pi \rightarrow \pi^*$)	3.81	0.0002	
7^3B_{3g} ($\pi \rightarrow \pi^*$)	3.93	0.0003	
6^3A_g ($\pi \rightarrow \pi^*$)	3.96	0.0947	
8^3B_{3g} ($\pi \rightarrow \pi^*$)	4.09	0.4769	
7^3A_g ($\pi \rightarrow \pi^*$)	4.23	0.6829	4.00[b]
9^3B_{3g} ($\pi \rightarrow \pi^*$)	4.29	0.1819	
2^3B_{1g} ($\pi \rightarrow \pi^*$)	4.50	0.0008	

[a] References 11, 46. [b] Reference 10.

Note that the predicted oscillator strengths for bands I and II are consistent with the observed intensity (see Figure 2 and Table 5). The next three states at 2.13, 2.29, and 2.43 eV (2^3B_{3g}, 2^3A_g, and 1^3B_{1g}) are not observed experimentally. These bands lie between the two more intense regions, and their intensities are too small to be visible. The 3^3B_{3g}, 3^3A_g, and 4^3B_{3g} states are assigned to band III at 2.82 eV. Again, the predicted oscillator strengths for these states appear to be consistent with the observed intensity and broadness of this band (see Figure 2 and Table 5). The most intense band with an observed maximum at 2.96 eV is likely composed of the 4^3A_g with contributions from the nearby 5^3B_{3g} state. These assignments leave band V at 3.23 eV to be assigned to the 6^3B_{3g} state with a computed excitation energy of 3.54 eV and a corresponding oscillator strength of 0.55. We note that the computed oscillator strength of band V (6^3B_{3g}) is larger than the oscillator strength assigned to band IV. The observed intensity of band IV, therefore, can be interpreted as borrowing intensity from the lower and higher energy transitions, which is consistent with the broadness of this band. The next two states, 5^3A_g and 7^3B_{3g}, have very small oscillator strengths. Therefore, the band with a maximum at 4.0 eV, reported by Radziszewski et al.,[10] is assigned to the 6^3A_g, 8^3B_{3g}, 7^3B_{3g}, and 9 $^3B_{3g}$ states, which accounts for its broadness. This high-energy region of the T−T spectrum is predicted to be the most intense, with a sum of oscillator strengths of 1.44. Further experimental work on the T−T spectrum of PH_2 would be required to verify the TDDFT results for the VI band because the differential spectrum reported by Radziszewski et al.[10] did not yield an absolute intensity.

TABLE 6: Dipole-Allowed T−T Excitation Energies (in eV) and Oscillator Strengths for β-Halogenated Free-Base Porphyrins

	β-PH_2F_8		β-PH_2Cl_8		β-PH_2Br_8	
transition	*E*	*f*	*E*	*f*	*E*	*f*
1^3A_g ($\pi \rightarrow \pi^*$)	1.26	0.0078	1.31	0.0100	1.29	0.0109
1^3B_{3g} ($\pi \rightarrow \pi^*$)	1.65	0.0036	1.56	0.0014	1.50	0.0029
2^3B_{3g} ($\pi \rightarrow \pi^*$)	1.97	0.0340	1.81	0.0716	1.77	0.0812
2^3A_g ($\pi \rightarrow \pi^*$)	2.25	0.0001	2.15	0.0011	2.12	0.0010
1^3B_{1g} ($\pi \rightarrow \pi^*$)	2.34	0.0006	2.35	0.0005	2.32	0.0005
3^3B_{3g} ($\pi \rightarrow \pi^*$)	2.66	0.0127	2.51	0.0245	2.46	0.0320
3^3A_g ($\pi \rightarrow \pi^*$)	2.68	0.0258	2.55	0.0209	2.45	0.0238
4^3B_{3g} ($\pi \rightarrow \pi^*$)	2.82	0.0296	2.69	0.0238	2.66	0.0234
5^3B_{3g} ($\pi \rightarrow \pi^*$)	2.93	0.0066	2.80	0.0291	2.76	0.0351
4^3A_g ($\pi \rightarrow \pi^*$)	3.21	0.1765	3.06	0.3583	3.01	0.4022
6^3B_{3g} ($\pi \rightarrow \pi^*$)	3.34	0.1320	3.19	0.2182	3.10	0.2391
5^3A_g ($\pi \rightarrow \pi^*$)	3.43	0.0770	3.34	0.0018	3.27	0.0001
7^3B_{3g} ($\pi \rightarrow \pi^*$)	3.55	0.0022	3.34	0.0025	3.25	0.0041
6^3A_g ($\pi \rightarrow \pi^*$)	3.56	0.0461	3.40	0.1308	3.33	0.1321
8^3B_{3g} ($\pi \rightarrow \pi^*$)	3.90	0.1868	3.61	0.2283	3.49	0.2833
9^3B_{3g} ($\pi \rightarrow \pi^*$)	3.94	1.0190	3.71	0.9128	3.58	0.5667
7^3A_g ($\pi \rightarrow \pi^*$)	4.19	0.8087				

2. $^3\beta$-PH_2X_8. The computed T−T excitation energies and oscillator strengths for β-PH_2X_8 are listed in Table 6. An inspection of the excitation energies and oscillator strengths (cf. Tables 5 and 6) reveals that β-halogenation significantly changes the T−T spectrum of porphin in both color and intensity. Most of the dominant features in the spectra of β-halogenated porphyrins retain the assigned symmetry of the parent PH_2. The assigned symmetry of a few dominant bands in PH_2 changes upon β-halogenation. The most intense band in both β-PH_2F_8 and β-PH_2Cl_8, for example, corresponds to 9^3B_{3g} rather than 7^3A_g (band VI) as in PH_2. The computed excitation energy and oscillator strength for the 9^3B_{3g} band in PH_2 are 4.29 eV and 0.18, respectively. This band is red-shifted by 0.35, 0.58, and 0.65 eV upon fluorination, chlorination, and bromination, respectively. The oscillator strength of the 9^3B_{3g} band is increased by 0.4−0.8 after halogenation. In a similar β-halogenation trend, the excitation energy of the 6^3B_{3g} state (band V) is progressively red-shifted upon going down the periodic table. However, in contrast to band VI, the oscillator strength of band V is predicted to significantly (0.3−0.4) decrease in magnitude. Interestingly, band VI is predicted to shift only slightly to the red (about 0.2 eV) for β-PH_2X_8 in comparison to PH_2. Fluorination is predicted to reduce the oscillator strength of band IV by a factor of 2, while chlorination and bromination increase it slightly. In band III of the PH_2 spectrum, which has contributions from the 3^3B_{3g} and 3^3A_g states with a gap of 0.2 eV, these states become nearly degenerate in β-PH_2X_8 due to the large red-shift of the 3^3A_g band upon β-halogenation. When PH_2 is β-brominated, the energy order of the 3^3B_{3g} and 3^3A_g states is reversed. The oscillator strengths of the 3^3B_{3g} and 3^3A_g states (band III) are not significantly affected by β-halogenation. The low-energy states are also perturbed greatly by β-halogen substituents. Energetically, the first allowed band is red-shifted by about 0.4 eV. However, the oscillator strengths of the first excited state for β-PH_2X_8 are not significantly different in comparison to those of PH_2.

C. Nonlinear Absorption. To provide an estimate of the nonlinear absorption spectral range for the dyes, their ground-state spectra are computed at the same level of theory. The results, summarized in Tables 7−9 and Figures 3−6, extend to the higher energy region which has not been considered previously.[21] In addition, the more economical local and

TABLE 7: Dipole-Allowed Ground-State Excitation Energies (in eV) for Free-Base Porphin

state[a]	B3LYP	B3P86	BP86	PW91	LSDA	BP[b]	SAC[c]	CC[d]	PT2[e]	exp[f]
1^1B_{1u} (Q_{II})	2.28	2.29	2.18	2.18	2.18	2.16	1.77	1.75	1.63	1.98
1^1B_{2u} ($Q_{\perp}$)	2.44	2.46	2.31	2.31	2.31	2.29	2.01	2.40	2.11	2.42
2^1B_{1u} (B_{II})	3.34	3.35	3.01	3.00	3.00	3.01	3.47	3.47	3.12	3.33
2^1B_{2u} ($B_{\perp}$)	3.51	3.52	3.04	3.04	3.04	2.98	3.73	3.62	3.08	3.33
3^1B_{2u} (N_{II})	3.77	3.78	3.47	3.47	3.47	3.47	4.20	4.06	3.53	3.65
3^1B_{1u} ($N_{\perp}$)	3.87	3.88	3.54	3.54	3.54	3.41	4.38	4.35	3.42	3.65
1^1B_{3u}	4.13	4.12	3.37	3.36	3.36	3.34	4.63	4.56		
4^1B_{2u} (L_{II})	4.36	4.37	3.80	3.78	3.80	3.77	5.15	5.00	3.96	4.25
4^1B_{1u} ($L_{\perp}$)	4.47	4.48	3.80	3.78	3.80	3.76	5.44	5.17	4.04	4.67
4^1B_{1u} (M_{II})	5.19	5.20	4.38	4.37	4.37			6.07		5.50

[a] In our coordinate system (IUPAC), the *y*-axis is perpendicular to inner N−H bonds and *yz* is taken as the σ_h plane. [b] Reference 47. [c] Reference 50. [d] Reference 49. [e] Reference 48. [f] Data taken in gas phase from reference 51.

TABLE 8: Dipole-Allowed Ground-State Oscillator Strengths for Free-Base Porphin

state[a]	B3LYP	B3P86	BP86	PW91	LSDA	BP[b]	SAC[c]	CC[d]	PT2[e]	exp[f]
1^1B_{1u} (Q_{II})	< 0.0001	< 0.0001	0.0011	0.0011	0.0014	0.01	0.003	< 0.001	0.004	0.01
1^1B_{2u} ($Q_{\perp}$)	< 0.0001	< 0.0001	0.0006	0.0006	0.0008	0.0005	0.013	0.016	0.002	0.06
2^1B_{1u} (B_{II})	0.4188	0.4226	0.1122	0.1123	0.1048	0.1338	0.772	1.03	0.911	1.15
2^1B_{2u} ($B_{\perp}$)	0.6306	0.6314	0.0271	0.0272	0.0237	0.04		1.42	0.704	
3^1B_{2u} (N_{II})	0.5094	0.5073	0.8437	0.8417	0.8147	0.7293	1.620	0.71	0.458	< 0.1
3^1B_{1u} ($N_{\perp}$)	0.7768	0.7744	0.7317	0.7305	0.7072	0.8962		0.44	0.833	
1^1B_{3u}	0.0015	0.0015	0.0008	0.0008	0.0008	0.0005	1.320	0.004		
4^1B_{2u} (L_{II})	0.1209	0.1251	0.1567	0.1561	0.1825	0.1272	0.339	0.20	0.341	~ 0.1
4^1B_{1u} ($L_{\perp}$)	0.1145	0.1172	0.2136	0.2165	0.2530	0.1688		0.410	0.202	
4^1B_{1u} (M_{II})	0.1430	0.1426	0.2540	0.2556	0.2515			0.190		~ 0.3

[a] In our coordinate system (IUPAC), the *y*-axis is perpendicular to inner N−H bonds and *yz* is taken as the σ_h plane. [b] Reference 47. [c] Reference 50. [d] Reference 49. [e] Reference 48. [f] Data taken in gas phase from reference 51.

TABLE 9: Dipole-Allowed Ground Excitation Energies (in eV) and Oscillator Strengths for β-Halogenated Free-Base Porphyrins[a]

	β-PH_2F_8		β-PH_2Cl_8		β-PH_2Br_8	
states	*E*	*f*	*E*	*f*	*E*	*f*
1^1B_{1u} (Q_{II})	2.31	0.0001	2.21	0.0012	2.19	0.0024
1^1B_{2u} ($Q_{\perp}$)	2.49	0.0007	2.37	0.0067	2.34	0.0110
2^1B_{1u} (B_{II})	3.06	0.0579	2.96	0.1221	2.90	0.1252
2^1B_{2u} ($B_{\perp}$)	3.23	0.0131	3.12	0.0308	3.05	0.0278
3^1B_{2u} (N_{II})	3.73	1.1493	3.46	1.2178	3.37	1.2443
3^1B_{1u} ($N_{\perp}$)	3.78	1.2397	3.54	1.3717	3.45	1.4254
1^1B_{3u}	4.15	0.0016	4.05	0.0013	3.98	0.0011
4^1B_{2u} (L_{II})	3.89	0.1522	3.68	0.2052	3.56	0.2267
4^1B_{1u} ($L_{\perp}$)	3.99	0.0840	3.71	0.0185	3.58	0.0010

[a] The Q, B, N, and L labels, adapted for β-PH_2X_8, designate energy orders, not excitation origins.

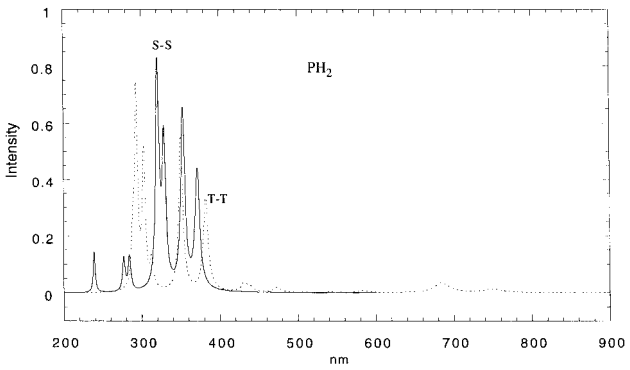

Figure 3. Ground (solid line) and triplet−triplet (dashed line) absorption spectra of PH_2.

nonhybrid functionals have been used to compute the spectrum of PH_2 in order to assess their applicability. We discuss first the effects of various functionals on the ground-state spectrum of PH_2, then the spectra of β-PH_2X_8, and finally the nonlinear absorption of these compounds. For PH_2, detailed comparisons of the TDDFT spectrum with experiment and other methods

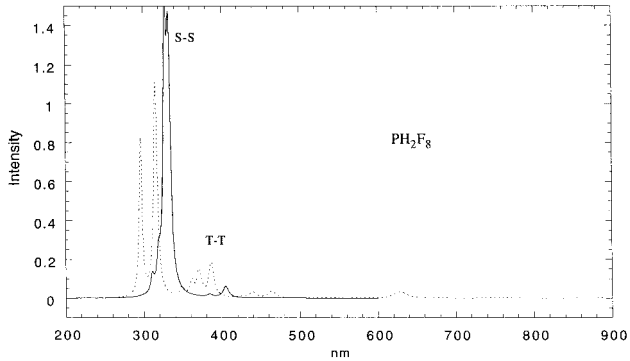

Figure 4. Ground (solid line) and triplet−triplet (dashed line) absorption spectra of β-PF_8H_2.

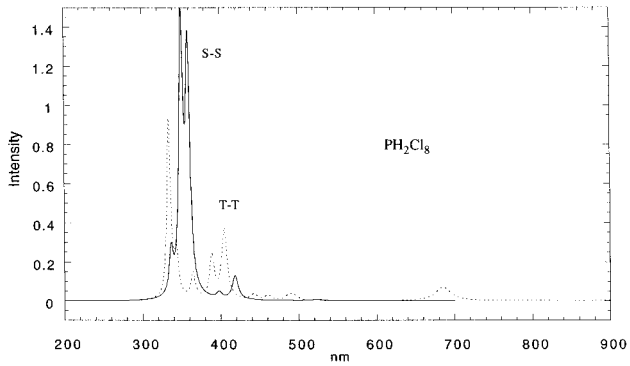

Figure 5. Ground (solid line) and triplet−triplet (dashed line) absorption spectra of β-PCl_8H_2.

have been given elsewhere.[21,24,47] We concentrate on key features that are related to the nonlinear absorption. It is clear from Tables 7 and 8 that the excitation energies and oscillator strengths are not significantly different among the local and nonhybrid potentials. The values predicted by the hybrid functionals appear to be more consistent with experiment through a wider spectral range than those predicted by the

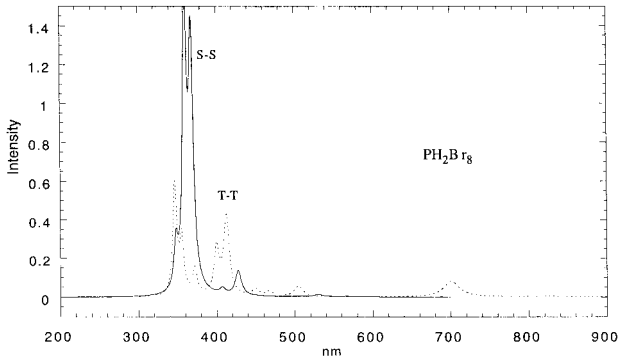

Figure 6. Ground (solid line) and triplet−triplet (dashed line) absorption spectra of β-PBr_8H_2.

nonhybrid and local functionals (see Tables 7 and 8). These general features appear to be more closely connected with the functionals since similar results have been obtained with larger Slater type basis sets.[47] The nonhybrid and local functionals significantly underestimate the oscillator strengths of the two B bands. Large deviations (ca. 0.5−1.1 eV) in excitation energy are also observed for the high-energy bands. These large errors are alleviated by the B3LYP and B3P86 hybrid functionals, which rival the multireference perturbation theory (PT2) and couple cluster (SAC-CI and CC) results in their quality.[48−50]

In porphyrins, nonlinear absorption derives from T−T excitations due to fast intersystem crossing. This type of photoinduced absorption, the so-called reverse saturable absorption, occurs when the excited-state absorption cross section is larger than its ground-state counterpart for a given wavelength. The spectral regions of strong NLA, therefore, are off-resonance in the ground-state spectrum. For PH_2, the optimal spectral windows with strong NLA appear to be on the low-energy side of the $B_{||}$ band and between the $N_\perp$ and $L_{||}$ bands. In β-PH_2X_8, the B bands are red-shifted and their intensities are significantly reduced (cf. Figures 3−6 and Table 9). Their spectral windows for NLA, therefore, are predicted to be broad for the low-energy region. In the high-energy regions of the ground-state spectra of β-PH_2X_8, the L bands are shifted closer to the more intense N bands and are overlapped with the T−T bands. However, NLA is expected to be strong, due to the large increase in oscillator strengths for the T−T bands in this region (see Figures 4−6).

IV. Summary and Conclusions

DFT and TDDFT calculations have been carried out to examine the structures, energetics, and excitation energies of $^3PH_2$ and its β-octahalogenated derivatives (β-PX_8H_2; X = F, Cl, Br). Two stable electronic states within the D_{2h} point group were located. The lowest triplet state, $1^3B_{2u}(b_{3u} \otimes b_{1g})$, is of $Q_\perp$ origin; the T_2 state is of $Q_{||}$ origin and is 0.36 eV higher in energy. The predicted S_0-T_1 splitting of 1.42 eV compares well with the experimental phosphorescence value of 1.58 eV reported by Gouterman and Khalil.[8] The predicted electronic and spatial symmetry of the T_1 state supports the electron spin resonance results.[9] The computed T−T spectrum of $^3PH_2$ accounts for the observed band maxima and their broadening. In the absence of experimental data, the computed ground and T−T spectra provide estimates for the nonlinear absorption windows for β-PX_8H_2. In addition, the results for β-PX_8H_2 provide the basic data for a quantitative account of substituent effects for the more complex phenylated and halogenated porphyrins that have been shown to exhibit significant NLA enhancement in comparison to the corresponding unsubstituted species.[3]

Acknowledgment. These calculations were performed on computers at the Aeronautical Systems Center (ASC) Major Shared Resource Center (MSRC). The support provided by the ASC MSRC Service Center is greatly appreciated. This work was supported by the Air Force Office of Scientific Research.

Supporting Information Available: A listing of optimized geometries (Cartesian coordinates). This material is available free of charge via the Internet at http://pubs.acs.org.

References and Notes

(1) Bonnett, R. *Chem. Soc. Rev.* **1995**, *24*, 19.
(2) Mansour, K.; Alvarez, D., Jr.; Perry, K. J.; Choong, I.; Marder, S. R.; Perry, J. W. *Proc. SPIE-Int. Soc. Opt. Eng.* **1993**, *1853*, 132.
(3) Su, W.; Cooper, T. M.; Brant, M. C. *Chem. Mater.* **1998**, *10*, 1212.
(4) Qureshi, F. M.; Martin, S. J.; Long, X.; Bradley, D. D. C.; Henari, F. Z.; Blau, W. J.; Smith, E. C.; Wang, C. H.; Kar, A. K.; Anderson, H. L. *Chem. Phys.* **1998**, *231*, 87.
(5) Stiel, H.; Volkmer, A.; Ruckmann, I.; Zeug, A.; Ehrenberg, B.; Roder, B. *Opt. Commun.* **1998**, *155*, 135.
(6) Seto, J.; Tamura, S.; Asai, N.; Kishii, N.; Kijima, Y.; Matsuzawa, N. *Pure Appl. Chem.* **1996**, *68*, 1429.
(7) Gradyushko, A. T.; Tsvirko, M. P. *Opt. Spectrosc.* **1971**, *31*, 291.
(8) Gouterman, M.; Khalil, G.-E. *J. Mol. Spectrosc.* **1974**, *53*, 88.
(9) van Dorp, W. G.; Soma, M.; Kooter, J. A.; van der Waals, J. H. *Mol. Phys.* **1974**, *28*, 1551.
(10) Radziszewski, J. G.; Waluk, J.; Michl, J. *J. Phys. Chem.* **1991**, *95*, 1963.
(11) Sapunov, V. V.; Solov'ev, K. N.; Tsvirko, M. P. *Zh. Prikl. Spektrosk.* **1974**, *21*, 667.
(12) Weiss, C.; Kobayashi, H.; Gouterman, M. *J. Mol. Spectrosc.* **1965**, *16*, 415.
(13) Langhoff, S. R.; Davidson, E. R.; Gouterman, M.; Leenstra, W. R.; Kwiram, A. D. *J. Chem. Phys.* **1975**, *62*, 169.
(14) Kooter, J. A.; van der Waals, J. H.; Knop, J. V. *Mol. Phys.* **1979**, *37*, 1015.
(15) van der Poel, W. A. J. A.; Singel, D. J.; Schmidt, J.; van der Waals, J. H. *Mol. Phys.* **1983**, *49*, 1017.
(16) Gouterman, M. *J. Chem. Phys.* **1960**, *33*, 1523.
(17) Baraldi, I.; Carnevali, A.; Ponterini, G.; Vanossi, D. *J. Mol. Struct. (THEOCHEM)* **1995**, *333*, 121.
(18) Kozlowski, P. M.; Zgierski, M. Z.; Pulay, P. *Chem. Phys. Lett.* **1995**, *247*, 379.
(19) Kozlowski, P. M.; Jarzecki, A. A.; Pulay, P. *J. Phys. Chem.* **1996**, *100*, 7007.
(20) Baker, J.; Kozlowski, P. M.; Jarzecki, A. A.; Pulay, P. *Theor. Chim. Acta* **1997**, *97*, 59.
(21) Nguyen, K. A.; Day, P. N.; Pachter, R. *J. Chem. Phys.* **1999**, *110*, 9135.
(22) Bauernschmitt, R.; Ahlrichs, R. *Chem. Phys. Lett.* **1996**, *256*, 454.
(23) Casida, M.; Jamorski, C.; Casida, K. C.; Salahub, D. R. *J. Chem. Phys.* **1998**, *108*, 4439.
(24) Stratmann, R. E.; Scuseria, G. E.; Frisch, M. J. *J. Chem. Phys.* **1998**, *109*, 8218.
(25) Nguyen, K. A.; Day, P. N.; Pachter, R. *J. Phys. Chem.* **1999**, *103*, 7378.
(26) Ghosh, A. *J. Am. Chem. Soc.* **1995**, *117*, 4691.
(27) Ghosh, A.; Vangberg, T. *Theor. Chim. Acta* **1997**, *97*, 134.
(28) Bonnet, R.; Harriman, A.; Kozyrev, A. *J. Chem. Soc., Faraday Trans.* **1992**, *88*, 763.
(29) Kohn, W.; Sham, L. J. *Phys. Rev. A* **1965**, *140*, 1133.
(30) Ditchfield, R.; Hehre, W. J.; Pople, J. A. *J. Chem. Phys.* **1971**, *54*, 724.
(31) Hehre, W. J.; Ditchfield, R.; Pople, J. A. *J. Chem. Phys.* **1972**, *56*, 2257.
(32) Stevens, W. J.; Basch, H.; Krauss, M. *J. Chem. Phys.* **1984**, *81*, 6026.
(33) Stevens, W. J.; Basch, H.; Krauss, M.; Jasien, P. *Can. J. Chem.* **1992**, *70*, 612.
(34) Becke, A. D. *J. Chem. Phys.* **1993**, *98*, 5648.
(35) Becke, A. D. *Phys. Rev. A* **1988**, *38*, 3098.
(36) Lee, C.; Yang, W.; Parr, R. G. *Phys. Rev. B: Condens. Matter* **1988**, *37*, 785.
(37) Pople, J. A.; Nesbet, R. K. *J. Chem. Phys.* **1959**, *22*, 571.
(38) Rothaan, C. C. J. *Rev. Mod. Phys.* **1951**, *23*, 69.
(39) Baker, J.; Scheiner, A.; Andzelm, J. *Chem. Phys. Lett.* **1993**, *216*, 380.

(40) Frisch, M. J.; Trucks, G. W.; Schlegel, H. B.; Scuseria, G. E.; Robb, M. A.; Cheeseman, J. R.; Zakrzewski, V. G.; Montgomery, J. A.; Stratmann, R. E.; Burant, J. C.; Dapprich, S.; Millam, J. M.; Daniels, A. D.; Kudin, K. N.; Strain, M. C.; Farkas, O.; Tomasi, J.; Barone, V.; Cossi, M.; Cammi, R.; Mennucci, B.; Pomelli, C.; Adamo, C.; Clifford, S.; Ochterski, J.; Petersson, G. A.; Ayala, P. Y.; Cui, Q.; Morokuma, K.; Malick, D. K.; Rabuck, A. D.; Raghavachari, K.; Foresman, J. B.; Cioslowski, J.; Ortiz, J. V.; Stefanov, B. B.; Liu, G.; Liashenko, A.; Piskorz, P.; Komaromi, I.; Gomperts, R.; Martin, R. L.; Fox, D. J.; Keith, T.; Al-Laham, M. A.; Peng, C. Y.; Nanayakkara, A.; Gonzalez, C.; Challacombe, M.; Gill, P. M. W.; Johnson, B. G.; Chen, W.; Wong, M. W.; Andres, J. L.; Head-Gordon, M.; Replogle, E. S.; Pople, J. A. *Gaussian 98*, revision A.7; Gaussian, Inc: Pittsburgh, PA, 1998.

(41) Vosko, S. H.; Wilk, L.; Nusair, M. *Can. J. Phys.* **1980**, *58*, 1200.

(42) Perdew, J. P. *Phys. Rev. B: Condens. Matter* **1986**, *23*, 8822.

(43) Perdew, J. P.; Wang, Y. *Phys. Rev. B: Condens. Matter* **1992**, *45*, 13244.

(44) Krishnan, R.; Binkley, J. S.; Seeger, R.; Pople, J. A. *J. Chem. Phys.* **1980**, *72*, 650.

(45) Clark, T. C., J.; Spitznagel, G. W.; Schleyer, P. v. R. *J. Comput. Chem.* **1983**, *4*, 294.

(46) Carmichael, I.; Gordon, H. L. *J. Phys. Chem. Ref. Data* **1986**, *15*, 1.

(47) van Gisbergen, S. J. A.; Ricciardi, A. R.; Baerends, E. J. *J. Phys. Chem.* **1999**, *111*, 2499.

(48) Serrano-Andres, L.; Merchan, M.; Rubio, M.; Roos, B. O. *Chem. Phys. Lett.* **1998**, *295*, 195.

(49) Gwaltney, S. R.; Bartlett, R. J. *J. Chem. Phys.* **1998**, *108*, 6790.

(50) Tokita, Y.; Hasegawa, J.; Nakatsuji, H. *J. Phys. Chem.* **1998**, *102*, 1843.

(51) Edwards, L.; Dolphin, D. H.; Gouterman, M.; Adler, A. D. *J. Mol. Spectrosc.* **1971**, *38*, 16.